


Prdm9 Intersubspecific Interactions in Hybrid Male Sterility of House Mouse

Amisa Mukaj,^{†,1} Jaroslav Piálek,^{†,2} Vladana Fotopulosova,¹ Andrew Parker Morgan,³ Linda Odenthal-Hesse,⁴ Emil D. Parvanov,^{*,1} and Jiri Forejt ^{*,1}

¹Department of Mouse Molecular Genetics, Institute of Molecular Genetics of the Czech Academy of Science, Vestec, Czech Republic

²Research Facility Studenec, Institute of Vertebrate Biology of the Czech Academy of Sciences, Brno, Czech Republic

³Department of Pediatrics, Duke University Hospital, Durham, NC

⁴Department of Evolutionary Genetics, Max Planck Institute for Evolutionary Biology, Ploen, Germany

[†]These authors contributed equally to this work.

*Corresponding authors: E-mails: jforejt@img.cas.cz; emil.parvanov@img.cas.cz.

Associate editor: John True

Abstract

The classical definition posits hybrid sterility as a phenomenon when two parental taxa each of which is fertile produce a hybrid that is sterile. The first hybrid sterility gene in vertebrates, *Prdm9*, coding for a histone methyltransferase, was identified in crosses between two laboratory mouse strains derived from *Mus mus musculus* and *M. m. domesticus* subspecies. The unique function of PRDM9 protein in the initiation of meiotic recombination led to the discovery of the basic molecular mechanism of hybrid sterility in laboratory crosses. However, the role of this protein as a component of reproductive barrier outside the laboratory model remained unclear. Here, we show that the *Prdm9* allelic incompatibilities represent the primary cause of reduced fertility in intersubspecific hybrids between *M. m. musculus* and *M. m. domesticus* including 16 *musculus* and *domesticus* wild-derived strains. Disruption of fertility phenotypes correlated with the rate of failure of synapsis between homologous chromosomes in meiosis I and with early meiotic arrest. All phenotypes were restored to normal when the *domesticus Prdm9^{dom2}* allele was substituted with the *Prdm9^{dom2H}* humanized variant. To conclude, our data show for the first time the male infertility of wild-derived *musculus* and *domesticus* subspecies F1 hybrids controlled by *Prdm9* as the major hybrid sterility gene. The impairment of fertility surrogates, testes weight and sperm count, correlated with increasing difficulties of meiotic synapsis of homologous chromosomes and with meiotic arrest, which we suppose reflect the increasing asymmetry of PRDM9-dependent DNA double-strand breaks.

Key words: reproductive isolation, *Prdm9* polymorphism, meiotic chromosome synapsis, HORMAD2, synaptonemal complex.

Introduction

The biological species concept defines species as groups of interbreeding natural populations reproductively isolated from other such groups (Mayr 1963). One postzygotic reproductive isolation mechanism, the sterility of interspecific hybrids, has attracted human curiosity since Aristotle discussed the infertility of mules. Charles Darwin foresaw hybrid sterility as a by-product of evolution, rather than a naturally selected trait (Darwin 1859). To reconcile Darwinian evolution with genetics, Dobzhansky and Muller (Dobzhansky 1936, 1951; Muller 1942; Muller and Pontecorvo 1942) proposed a genetic model explaining hybrid sterility as an incompatibility between independently diverged genes. During the last 80 years, most of our genetic knowledge on hybrid sterility

in animals came from the studies of *Drosophila* species (Naveira and Maside 1998; Coyne and Orr 2004; Presgraves 2008; Maheshwari and Barbash 2011), nonetheless, the main principles of hybrid sterility proved valid for many other animal and plant species hybrids (Schilthuizen et al. 2011). These include Haldane's rule stating that the heterogametic (XY or ZW) sex is preferentially affected in hybrids (Haldane 1922), or the large X-effect (Coyne's rule) referring to the predominant role of the X chromosome in contrast to autosomes (Dobzhansky 1951; Forejt 1996; Coyne and Orr 2004; Good et al. 2008; Presgraves 2018), Perhaps surprisingly, given the extensive genetic studies in species such as fruit flies, yeasts, and house mice, the genetic architecture of hybrid sterility as well as the molecular mechanisms behind these rules remain

mostly unclear (reviewed in Maheshwari and Barbash [2011], Phifer-Rixey and Nachman [2015], Dion-Cote and Barbash [2017], Mack and Nachman [2017], Payseur et al. [2018]).

Although hybrid sterility usually behaves as a complex polygenic trait, a handful of discrete hybrid sterility and hybrid inviability genes such as *Odsh*, *JYAlpha*, *Hmr*, *Nup96*, and *Ovd* have been described mostly in *Drosophila* (Ting et al. 1998; Barbash et al. 2003; Presgraves et al. 2003; Masly et al. 2006; Phadnis and Orr 2009). Forejt and Ivanyi (1974) mapped the first hybrid sterility genetic locus in vertebrates (Hybrid sterility 1, *Hst1*) in crosses of wild male mice of the *Mus musculus musculus* (hereafter referred to as *musculus*) subspecies with females of laboratory inbred strains of the *Mus musculus domesticus* (hereafter *domesticus*) origin. Later, by positional cloning, they identified the *Hst1* locus with the *Prdm9* gene coding for PR/SET domain-containing 9 protein (Mihola et al. 2009). The current model of *Prdm9*-controlled hybrid sterility refers to male progeny of an intersubspecific cross of *musculus* wild-derived PWD strain females and C57BL/6J (hereafter B6) *domesticus* laboratory strain males. Hybrid descendants of the cross are viable and healthy individuals except that all males are completely sterile. The phenotype of hybrid sterility includes small testes, absence of sperm, meiotic arrest at the mid-to-late pachytene stage (Forejt 1996; Forejt et al. 2012), impairment of transcriptional inactivation of the sex chromosomes (MSCI), and incomplete meiotic chromosome synapsis (Forejt 1984; Bhattacharyya et al. 2013; Gregorova et al. 2018). Obeying Haldane's rule, the female hybrids are fertile, though with partially defective oogenesis (Bhattacharyya et al. 2014). In contrast to other mouse studies, which observed a complex polygenic nature often of dozens of hybrid incompatibilities (Tucker et al. 1992; Payseur et al. 2004; Macholan et al. 2007, 2011; Duvaux et al. 2011; Janoušek et al. 2012; Turner et al. 2012; Morgan et al. 2020), the genomic architecture of the F1 hybrid sterility of (PWD×B6)F1 males appears relatively straightforward. The three main components consist of the intersubspecific allelic combination *Prdm9*^{PWD/B6}, the PWD allelic form of the X-linked *Hstx2* locus (Storchova et al. 2004; Bhattacharyya et al. 2014; Lustyk et al. 2019), and the PWD/B6 heterozygosity of homeologous autosomes (homeologs are homologous autosomes from related (sub)species) (Gregorova et al. 2018).

PRDM9 is a histone methyltransferase enzyme that initiates meiotic recombination (Baudat et al. 2010; Myers et al. 2010; Parvanov et al. 2010) by directly binding DNA via its C-terminal zinc finger (ZnF) domain. The ZnF domain is highly polymorphic within and between mouse subspecies and determines the allelic specificity of PRDM9 DNA-binding sites. After binding to DNA, PRDM9 defines specific sites (hotspots) where meiotic recombination may occur (Hayashi and Matsui 2006; Smagulova et al. 2011; Wu et al. 2013; Baker et al. 2014; Eram et al. 2014; Powers et al. 2016) by inserting trimethylation marks on the lysine 4 and lysine 36 residues of histone 3 (H3K4me3 and H3K36me3). The PRDM9-marked hotspots guide SPO11 protein to induce programmed DNA double-strand breaks (DSBs) along the chromosomes, which are repaired by homologous recombination either as crossovers or noncrossovers (gene conversions) (for

review, see Hunter [2015] and Smith and Nambiar [2020]). The lack of PRDM9 leads to redistribution of recombination events toward the functional elements such as promoters that are also marked by H3K4me3 (Smagulova et al. 2016) resulting in sterility in both sexes (Hayashi and Matsui 2006) (but see Mihola et al. [2019]).

The molecular mechanism by which *Prdm9* acts as a mouse hybrid sterility gene is less clear. The “asymmetry-due-to erosion” hypothesis posits the differential erosion of PRDM9 binding sites in *musculus* and *domesticus* subspecies as the initial event (Davies et al. 2016). The evolutionary erosion is a well-documented feature of recombination as well as *Prdm9* hotspots in several species (Boulton et al. 1997; Myers et al. 2010; Baker et al. 2015). The erosion at the evolutionary scale is explained by biased gene conversion that favors repair using the template with lower PRDM9 affinity, because initiation of DNA DSBs is preferred at the PRDM9 binding sites with higher affinity. In this way, a subset of PRDM9 recognition sequences is gradually blurred in one subspecies but remains intact in the other. In (PWD×B6)F1 intersubspecific hybrids, the asymmetric hotspots occur predominantly on a “nonself chromosome” where the recognition motifs are intact; the PRDM9^{B6} hotspots appear mostly on PWD chromosomes and PRDM9^{PWD} hotspot on B6 chromosomes. It is presumed that the SPO11-induced DSBs at such asymmetric hotspots are difficult to repair from the homologous chromosome or are repaired using the sister chromatid as a template (Hinch et al. 2019), resulting in asynapsis and apoptosis. Many aspects of this “asymmetry-due-to erosion” hypothesis remain unsolved, such as the role of the second major hybrid sterility factor located within the X-linked *Hstx2* locus, the significance of “default,” *Prdm9*-independent hotspots (Hayashi and Matsui 2006; Smagulova et al. 2016), or the effect of PRDM9 binding sites within repetitive sequences (Yamada et al. 2017). However, several pieces of evidence supporting this idea have been gathered (Gregorova et al. 2018; Wang et al. 2018; Gergelits et al. 2019).

To sum up, the *Prdm9*-dependent model of hybrid sterility has all principal attributes of classical F1 hybrid sterility (Coyne and Orr 2004) including underdominance (*Prdm9* heterozygosity-dependent sterility), male-limited infertility following Haldane's rule, and the large X-effect reflected by the interacting X-linked *Hstx2* locus (Lustyk et al. 2019). However, virtually nothing is known about *Prdm9* allelic incompatibilities in the hybrids of wild mice, known to display a high level of intrasubspecific *Prdm9* polymorphism (Buard et al. 2014; Kono et al. 2014; Vara et al. 2019), an unorthodox feature for a hybrid sterility gene. To investigate the role of *Prdm9*-dependent reproductive isolation in natural mouse populations, we tested ten different *Prdm9* alleles from 16 European populations of *musculus* and *domesticus* subspecies for their effect on fertility of intersubspecific F1 hybrids. We found that aberrant synapsis of meiotic chromosomes is indeed a *Prdm9*-dependent trait negatively correlated with surrogate fertility phenotypes—number of produced sperm cells and testes weight. Moreover, despite a continuum of variation in fertility-related phenotypes, full hybrid sterility occurred when the asynapsis rate exceeded a certain

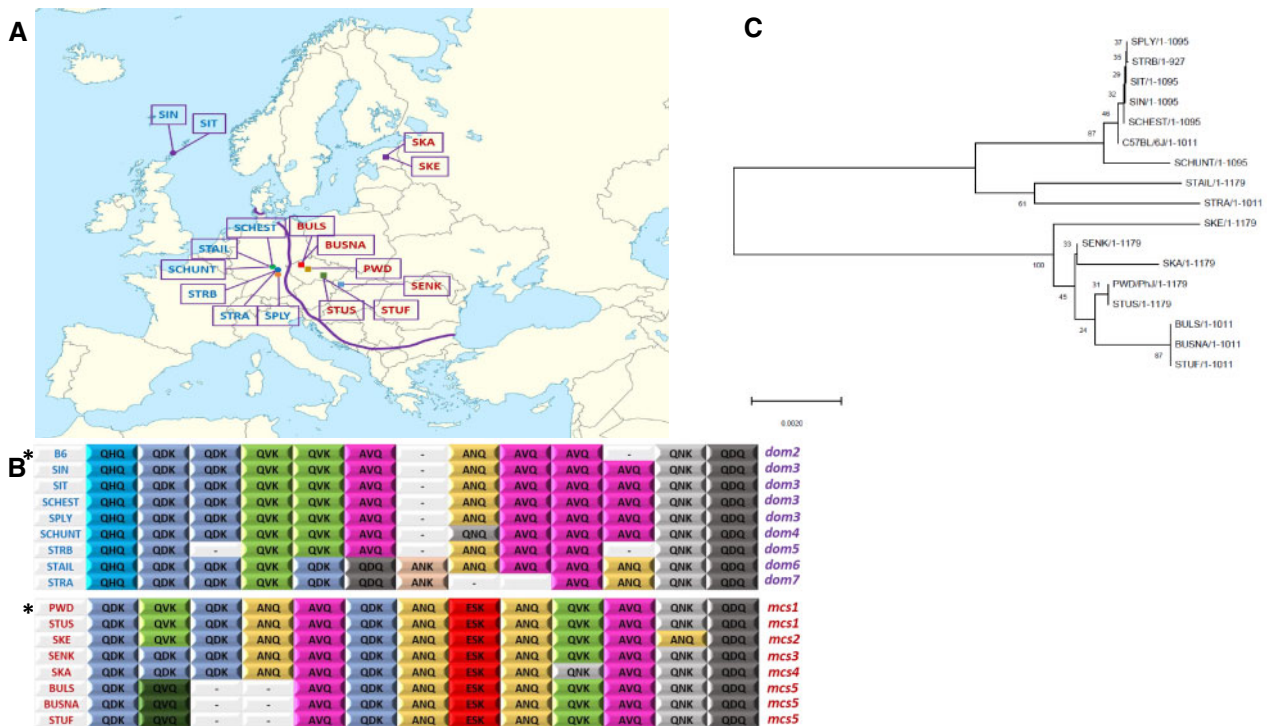


Fig. 1. Geographic distribution of founders of wild-derived strains and their *Prdm9* ZnF arrays. (A) Localities of origin of eight *musculus* (squares) and eight *domesticus* (circles) strains along the *musculus/domesticus* hybrid zone (Baird and Macholan 2012; Dureje et al. 2012; Macholan et al. 2019). *Musculus* strains: SKA, Kaerepere, Estonia; SKE, Keava, Estonia; BULS and BUSNA, Buškovice, Czech Republic; PWD, Kunratice (Prague), Czech Republic; STUF and STUS, Studenec, Czech Republic; SENK, Šenkvice, Slovak Republic. *Domesticus* strains: STRA and STRB, Straas, Bavaria, Germany; STAIL and SCHUNT, Schweben, Hessen, Germany; SPLY, Plöessen, Bavaria, Germany; SIN and SIT, Scar, Sanday Island, Orkneys, Scotland. The blank map of Europe by courtesy of Wikimedia Commons (https://en.wikipedia.org/wiki/File:Europe_blank_laea_location_map.svg#filehistory). (B) PRDM9 zinc finger arrays of all strains. The first, nonvariant ZnF separated from ZnF domain is not shown. Three DNA-binding amino acids represent each ZnF. Included are allelic variants of reference strains B6 and PWD. (C) Phylogenetic relationships between *Prdm9* alleles estimated using the neighbor-joining method in MEGA X (Kumar et al. 2018). The numbers next to each node represent bootstrapping values.

threshold level. Our results provide the first direct evidence that incompatibilities between *Prdm9* alleles segregating in natural populations can result in F1 hybrid sterility.

Results

Identification of Intersubspecific Introgressions in Genomes of Wild-Derived Strains

All 16 wild-derived mouse strains originated from founders trapped in Central and Western Europe (Gregorova and Forejt 2000; Pialek et al. 2007; Martinová et al. 2019) (see also Materials and Methods and <https://housemice.cz/en>; last accessed July 11, 2020). The sampling sites were located on both sides of the European natural hybrid zone separating *musculus* and *domesticus* subspecies (Macholán et al. 2007; Geraldès et al. 2008; Duvaux et al. 2011; Baird and Macholan 2012), whose genomes diverged ~ 0.5 Ma (She et al. 1990; Boursot et al. 1996; Salcedo et al. 2007; Geraldès et al. 2008) (fig. 1A). Since genomic introgression occurs in both directions across the hybrid zone (Payseur et al. 2004; Teeter et al. 2007; Dufkova et al. 2011; Macholan et al. 2011; Janoušek et al. 2012), we first searched for possible genomic admixtures from the other subspecies. Such introgressions could influence local meiotic pairing between *musculus* and *domesticus* homologs, as modeled by hybrids of the intersubspecific chromosome

substitution strains (Gregorova et al. 2018). To identify the introgressed genomic segments, we used a high-density SNP genotyping array (Morgan et al. 2015) in eight *musculus* and seven *domesticus* wild-derived inbred strains. The wild-derived PWD/Ph (hereafter PWD) and classical laboratory strain C57BL/6j (hereafter B6) inbred strains were included as a reference. The highest admixture of *musculus* in *domesticus* strains was 7.01% in the B6 reference strain; it is well known that most classical inbred strains, although primarily of *domesticus* ancestry, have significant *musculus* component (Yang et al. 2011). The remaining seven *domesticus* strains (SPLY, SIN, SIT, SCHUNT, STRB, STRA, STAIL) all showed $< 1\%$ of the genome (autosomes + X chromosome) of *musculus* ancestry (0.07–0.97%). The SPLY strain differs from other *domesticus* strains by the presence of a *musculus* Y chromosome, and C57BL/6j is confirmed to carry a different *musculus* Y chromosome (Nagamine et al. 1992; Morgan and Pardo-Manuel de Villena 2017) (supplementary table S1 and fig. S1, Supplementary Material online). The SCHEST strain became extinct before genotyping could be performed. Remarkably, many introgressed segments were found recurrently; seven *domesticus* strains (excluding B6 reference) displayed in total 73 *musculus* segments, of which 35 occurred only once and the remaining 38 consisted of 12 distinct segments shared by 2–5 strains (supplementary fig. S1 and table

S2, Supplementary Material online). Eight *musculus* strains displayed 91 islands of the *domesticus* sequence. Eighty-one occurred only once, whereas ten consisted of five distinct islands shared by two strains. These regions could represent introgression events that have risen to high frequency in source populations, or (less likely) artifacts in ancestry assignment. All *musculus* strains except PWD showed <1% (0.02–0.6%) of the *domesticus* ancestry. The PWD genome includes 4.89% (133.5 Mb) of *domesticus* segments, of which 26.52 and 44.2 Mb are situated on the chromosomes 9 and 14, respectively (supplementary table S3, Supplementary Material online, see also Yang et al. [2011]). Thus, besides these two PWD chromosomes, no chromosome in any other studied strain displayed >27-Mb introgression, a threshold previously shown to be sufficient for rescuing meiotic synapsis of interspecific homologs (Gregorova et al. 2018).

ZnF Sequence, Nomenclature, Geography, and Phylogeny of the Studied *Prdm9* Alleles

The PRDM9 ZnF haplotypes of individual wild-derived strains were identified after amplification and sequencing of PRDM9 exon12, which contains the entire ZnF array except for the first, invariant ZnF repeat. Sequences of individual ZnFs were translated, and three highly variable DNA-binding amino acids at positions –1, +3, and +6 (Oliver et al. 2009) were used to identify each ZnF type. Five distinct haplotypes were present in eight *musculus* strains, and five haplotypes in eight *domesticus* strains (fig. 1B). The PRDM9 ZnF sequences were deposited to GenBank under accession numbers MT252946–MT252960. To follow the official nomenclature (International Committee on Standardized Genetic Nomenclature for Mice; <http://www.informatics.jax.org/mgihome/nomen/index.shtml>; last accessed July 11, 2020), we applied serial numbers to the newly identified *Prdm9*^{msc#} *musculus* and *Prdm9*^{dom#} *domesticus* alleles. The only so far registered *musculus* allele *Prdm9*^{msc} (PWD/Ph inbred strain) was given number 1, *Prdm9*^{msc1}.

Only the PWD/Ph and STUS wild-derived *musculus* strains, from the localities Kunratice and Studenec, Czech Republic, carried the *Prdm9*^{msc1} allele (fig. 1B). Three other strains displayed variants of PRDM9^{msc1} protein, which we designated PRDM9^{msc2} and PRDM9^{msc3} and which differ only in a single ZnF (SKE strain from Estonia, substitution of QNK by ANQ in the 13th ZnF, and SENK strain from Slovakia, substitution of QVK by QDK in the third ZnF). The PRDM9^{msc4} differs by two ZnFs (SKA strain from Estonia—substitution of QVK by QDK in the third ZnF and QVK by QNK in the 11th ZnF). The remaining three *musculus* strains (BULS and BUSNA) carry the same *Prdm9*^{msc5} allele, which differs from *Prdm9*^{msc1} by deletion of sequence for the fourth and fifth ZnFs and by substitution of QVK by QVQ in the third ZnF (fig. 1B). Notably, all five substitutions but one occurred at the QVK ZnF, and always at amino acid positions responsible for DNA binding, namely positions +3 or +6 of the alpha-helix of the C2H2 ZnF.

The *Prdm9*^{dom2} *domesticus* allele present in the reference B6 strain and in many other laboratory inbred strains was absent among the eight *domesticus* wild-derived strains. The

allele most similar to *Prdm9*^{dom2} was *Prdm9*^{dom3} found in four wild-derived *domesticus* strains. The same allele has already been described in several laboratory inbred strains (C3H/HeJ, CBA/CaJ, NOD/LtJ, PERA/EiJ, and WSB/EiJ). The founders of strains carrying *Prdm9*^{dom3} came from Orkney Islands, UK (SIN and SIT); Bavaria, Germany (SPLY); and Hesse, Germany (SCHEST). SCHUNT, also from Hesse carries the *Prdm9*^{dom4}, which differs from *Prdm9*^{dom3} only at ZnF8 (substitution of ANQ by QNQ) (fig. 1B). The *Prdm9*^{dom5} allele (strain STRB) from Bavaria differs from *Prdm9*^{dom2} only by a deletion of the fourth ZnF. The remaining two alleles *Prdm9*^{dom6} (STAIL, Hesse) and *Prdm9*^{dom7} (STRA, Bavaria) appear the most distant from the *Prdm9*^{dom2} reference.

The *Prdm9*^{dom3} allele was the most frequent *domesticus* allele identified in two large-scale studies of wild mice, occurring in 23.1% (9/39) and 35% (7/20) cases in widely separated sites along the European hybrid zone (Buard et al. 2014; Kono et al. 2014). Admittedly, our choice of strains was not completely random, since SIN and SCHEST strains, which both turned out to be *Prdm9*^{dom3}, were sequenced based on our previous knowledge of male sterility of their hybrids (see below). The *Prdm9*^{msc1} allele of the PWD reference and STUS strains was the most common allele among the *musculus* samples (30%, 6/20) (Buard et al. 2014), though only in 7.4% (2/27) of mice in Eastern Europe and Asia screened in a previous (Kono et al. 2014).

The evolutionary relationships between the zinc finger arrays of *Prdm9* alleles of individual wild-derived strains were estimated using MEGA X (Kumar et al. 2018) (fig. 1C). The *musculus* alleles can be divided into two subgroups—the group of BULS, BUSNA, and STUF and the group of “PWD-like” alleles SKA, SKE, and SENK. In the *domesticus* group, STRA and STAIL alleles seem evolutionarily distant forming a separate group from the remaining alleles. The distribution of *musculus* and *domesticus* alleles respected the hybrid zone between both subspecies, but within each subspecies territory showed limited local clustering.

Prdm9 Controls Fertility Phenotypes of Intersubspecific Hybrids

Three main components, intersubspecific allelic heterozygosity *Prdm9*^{msc1/dom2}, *Hstx2*^{PWD} locus on Chromosome X, and F1 hybrid genetic background, define the genomic architecture of the (PWD×B6)F1 laboratory model of hybrid sterility (Bhattacharyya et al. 2013, 2014; Gregorova et al. 2018; Lustyk et al. 2019) (fig. 2A). To evaluate the general validity of this model for other wild-derived *musculus* *Prdm9*^{msc#} alleles, we designed crosses where *Hstx2*^{PWD} and *Prdm9*^{dom2} alleles remained constant, and the only variables in the F1 hybrid genome were the wild-derived *Prdm9*^{msc#} allele and the *musculus* portion of the genomic background (fig. 2B). The effect of a “humanized” *Prdm9*^{dom2H} allele (Davies et al. 2016) known to rescue sterility of (PWD×B6)F1 hybrids was assessed in hybrids with wild-derived *Prdm9*^{msc#} variants (fig. 2C). Similarly, to test *domesticus* *Prdm9* alleles, PWD females were crossed with the *domesticus* wild-derived males. In this cross, both *Hstx2*^{PWD} and *Prdm9*^{msc1} were controlled, whereas the wild-derived *Prdm9*^{dom#} and the *domesticus* part

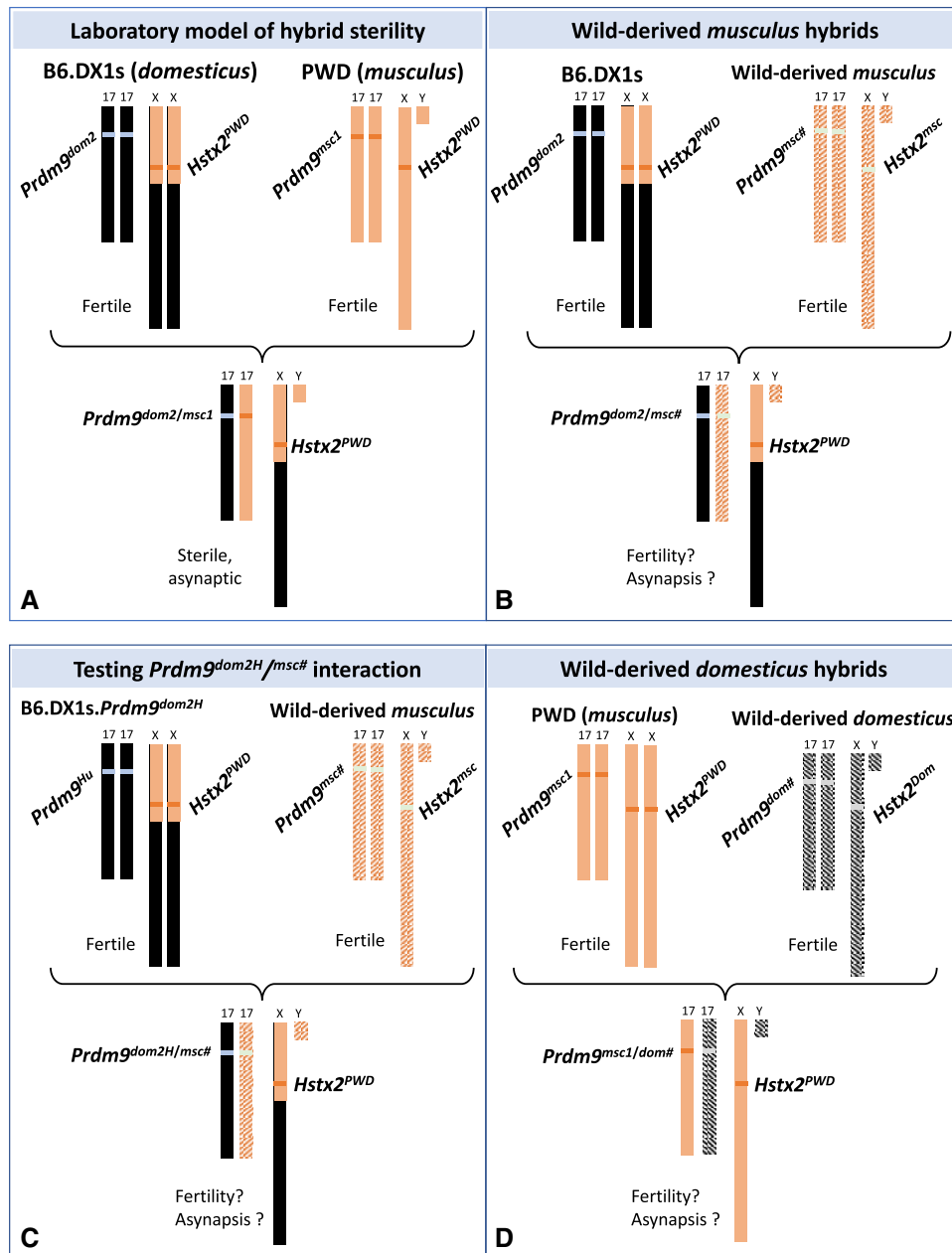


FIG. 2. Scheme of F1 hybrid genotypes to test the role of PRDM9 alleles in F1 hybrid fertility. (A) The laboratory model of (PWD×B6)F1 hybrid sterility. The first parent is female. Hybrid sterility depends on *Prdm9^{msc1/dom2}* heterozygosity, presence of PWD allele of Hybrid sterility X2 (*Hstx2^{PWD}*) on chromosome X and on interaction of homeologous (*domesticus/musculus*) autosomes. (B) The *Hstx2^{PWD}* and *Prdm9^{dom2}* alleles interact with the *Prdm9* allele from a wild-derived *musculus* in B6.DX1s×wild-derived *musculus* F1 hybrid. (C) The same cross as in (B) but *Prdm9^{dom2}* is replaced by humanized *Prdm9^{dom2H}*, known to restore *Prdm9*-dependent sterility. (D) The same *Prdm9* and *Hstx2* genotype as in (A) but *Prdm9^{dom2}* is replaced by a wild-derived *domesticus* allele.

of genetic background varied (fig. 2D). The synapsis of meiotic chromosomes was visualized by immunostaining of axial elements of synaptonemal complexes by antibody against SYCP3 protein on spermatocyte nuclei spreads. Furthermore, the HORMA domain-containing protein-2 (HORMAD2), which is a meiosis-specific protein known to accumulate on unsynapsed chromosome axes (Wojtasz et al. 2009) was used to visualize asynapsed homologs (Bhattacharyya et al. 2013, 2014; Gregorova et al. 2018). To score the synapsis failure, one asynapsis event was defined as

one HORMAD2 positive structure, mostly an unsynapsed univalent. Normal asynapsis events, namely HORMAD2 positive nonhomologous parts of X and Y sex chromosomes as well as the unpaired axial elements of cells at earlier stages (leptotene, zygotene) were not scored as asynapsis events. To differentiate between zygotene and pachytene stages of the first meiotic prophase, we utilized phosphorylated histone H2AX at Ser 139 (γ-H2AX) immunostaining (fig. 3). Phosphorylation of H2AX is an early mark of DNA DSBs. In wild-type spermatocytes, it decorates unsynapsed autosomal

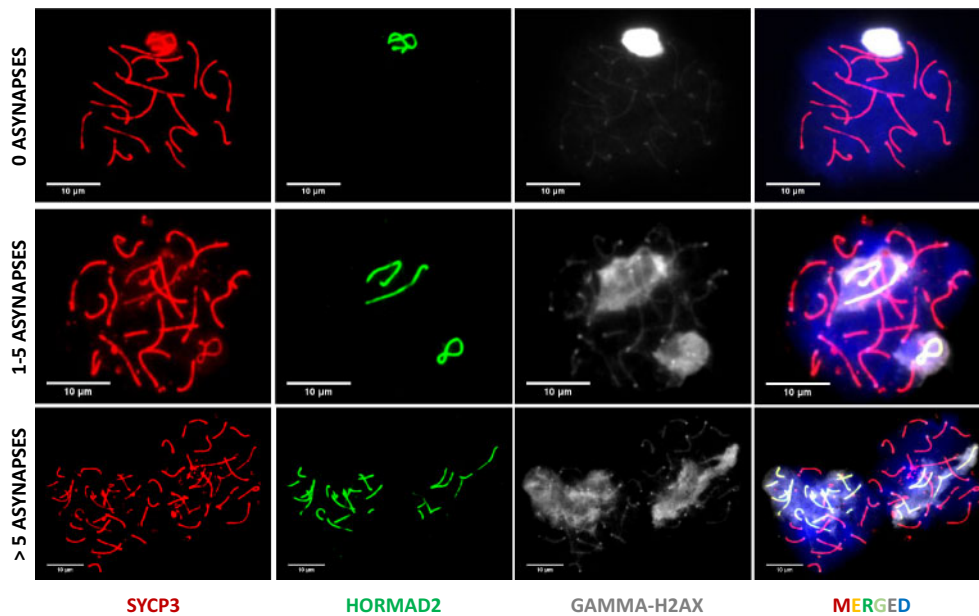


Fig. 3. Representative immunofluorescence images of chromosome synapsis in spreads of pachynema nuclei. Synaptonemal complexes are visualized by immunostaining SYCP3 protein (red), asynapsed parts of the XY sex chromosomes and unsynapsed autosomes are decorated by anti HORMAD2 antibody (green) and DNA is counterstained with DAPI (blue). The images illustrate a fully synapsed cell (top panel), where only the nonhomologous parts of sex chromosomes are decorated by HORMAD2 and the cells of two categories, 1–5 asynapses (middle panel) and >5 asynapses (bottom panel). One asynapsis is defined as one HORMAD2-stained structure, most often representing a univalent, an unpaired homolog.

stretches at the zygotene stage and transcriptionally inactive X and Y chromosomes engulfed within the XY (sex) body in the pachytene spermatocytes (Wojtasz et al. 2012). Altogether 10,333 immunostained pachynemas were analyzed, and relation between meiotic chromosome asynapsis rate and fertility phenotypes was studied.

The Wild-Derived *musculus* *Prdm9*^{msc#} Alleles Control Fertility Phenotypes of Hybrids

Females of congenic *domesticus* strain B6.PWD-Chr X.1s (hereafter B6.DX1s) carrying the hybrid sterility-augmenting *Hstx2*^{PWD} locus (Bhattacharyya et al. 2014; Lustyk et al. 2019) were crossed with males of the eight *musculus* wild-derived inbred strains to ensure the same *Hstx2* allele in hybrids. Their F1 hybrid male progeny was phenotyped at 60-day postpartum (dpp) by determining the absolute testes weight, the number of sperm cells in both epididymides, and asynapsis rate (see Materials and Methods for using absolute testes weight values). *Prdm9* alleles were determined after fertility data were obtained. Phenotyping of (B6.DX1s × *musculus*)F1 hybrids revealed a considerable variation between both fertility phenotypes and asynapsis rates, dependent on the wild-derived *Prdm9* allele. Besides the PWD reference strain, only STUS and SKE produced fully sterile hybrids (no sperm and >90% of asynapsed pachynemas). STUS was the only strain that shared the *Prdm9*^{msc1} allele with PWD (fig. 4A). The most related to *Prdm9*^{msc1} were the *Prdm9*^{msc2} and *Prdm9*^{msc3} alleles of SKE and SENK strains, which each showed a single ZnF substitution in their ZnF arrays. Following the predicted importance of ZnF3 to ZnF6 for specificity of the DNA-binding motif (Paigen and Petkov 2018), a single substitution

of ZnF at position 3 (QVK to QNK amino acid triplets) in *Prdm9*^{msc3} of the SENK strain was associated with restoration of full male fertility and only 8% of asynaptic pachynemas. In contrast, the SKE males with the substituted ZnF13 (QNK to ANQ) produced sterile hybrids with 0–0.17 × 10⁶ sperm cells, small testes, and 68.2% of pachynemas showing asynapsis (fig. 4A).

To further investigate the contribution of *Prdm9* to these fertility phenotype variations, we employed B6.DX1s mice with humanized *Prdm9*^{dom2H} gene. This engineered allele is identical with *Prdm9*^{dom2} except for the substituted sequence of the ZnF array coming from the human *PRDM9*^b ortholog. In (PWD × B6.*Prdm9*^{dom2H})F1 hybrid males, humanization of *Prdm9* improved symmetric binding of PRDM9 equally on paternal and maternal chromosomes and reversed their sterility (Davies et al. 2016). We used the B6.DX1s.*Prdm9*^{dom2H} mice with humanized *Prdm9*^{dom2H} and *Hstx2*^{PWD} locus to probe the involvement of *Prdm9* in fertility impairment of hybrids with wild-derived *musculus* strains. Provided that the low testes weight and sperm count were caused by *Prdm9*-unrelated hybrid sterility gene(s), the expected increase of symmetric PRDM9 binding caused by humanized allele should not improve the fertility scores. On the contrary, if the decreased fertility of hybrids is (predominantly) under the *Prdm9* control, the humanized allele should restore fertility to normal values. Indeed, in crosses of B6.DX1s.*Prdm9*^{dom2H} females with males of wild-derived *musculus* strains, we observed complete reversal of male sterility of PWD, STUS, and SKE hybrids and recovery of physiologically normal synapsis of homologous chromosomes (fig. 4A). The fertility

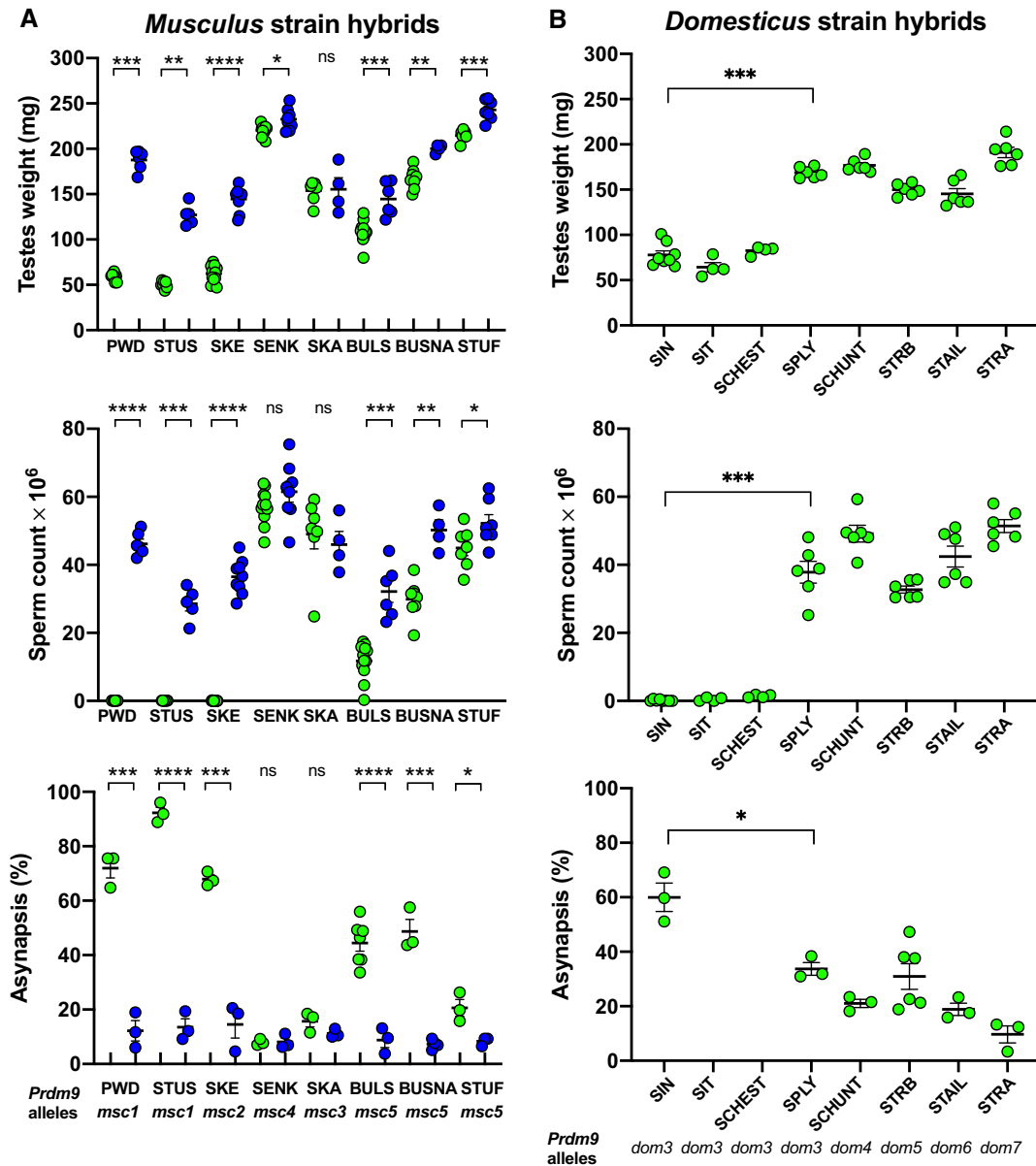


Fig. 4. Fertility phenotypes and chromosome pairing of intersubspecific mouse hybrids. (A) Hybrids from crosses of *musculus* wild-derived inbred strain males and B6.DX1s (green circles) or B6.DX1s. *Prdm9*^{dom2H} “humanized” *domesticus* females (blue circles). Only *Prdm9*^{msc1} and related *Prdm9*^{msc2} alleles support high asynapsis and full meiotic arrest or quasi sterility. The *Prdm9* control of fertility phenotypes is shown by improved meiotic chromosome pairing and fertility parameters in hybrids carrying humanized alleles compared with the *Prdm9*^{dom2} allele. (B) Hybrids of PWD *musculus* females and wild-derived *domesticus* males. All wild-derived strains that carry the *Prdm9*^{dom3} allele except for SPLY, produced sterile hybrids. Asynapsis rate was significantly higher in sterile SIN hybrids than in fertile SPLY carrying the same *Prdm9*^{dom3} allele. Significance of fertility improvement caused by the humanized *Prdm9* allele was evaluated by Mann–Whitney *U* test for testes weight and sperm count and by unpaired two-tailed *t*-test for asynapsis. *P* values <0.0001***, 0.0001–0.001**, 0.001–0.01**, 0.01–0.05*, >0.05 ns.

phenotypes of hybrids of the remaining five strains were improved proportionally to the degree of their spermatogenic damage. In all cases of lower sperm counts and testes weights in the (B6.DX1s \times *musculus*) hybrids, we saw an increase in sperm production after the *Prdm9*^{dom2} allele was replaced by the humanized one. The alleles of BULS and BUSNA showed a mean sperm count increase from 11.8 to 32.2 million and from 29.9 to 50.2 million, respectively. The asynapsis rates were lowered accordingly. In the case of SKE allele, asynapsis decreased from 68.0% down to 14.6%. The *Prdm9*^{dom2H} allele also reduced the mean asynapsis rate

of pachynemas in the hybrids of SKA (15.7–11.2%), BULS (from 44.4% to 8.8%), BUSNA (from 48.7% to 7.3%), and STUF (from 20.6% to 8.4%) strains. The reduction of the asynapsis rate coincided with a complete lack of cells with more than five asynapses along with a decrease of the cell population with one to six asynapses (fig 4A and supplementary fig. S2, Supplementary Material online).

We can conclude that the sterility of the studied F1 hybrids was *Prdm9*-dependent since the humanized *Prdm9* allele completely rescued meiotic pairing and spermatogenic arrest. The persisting differences in the testes weight and sperm

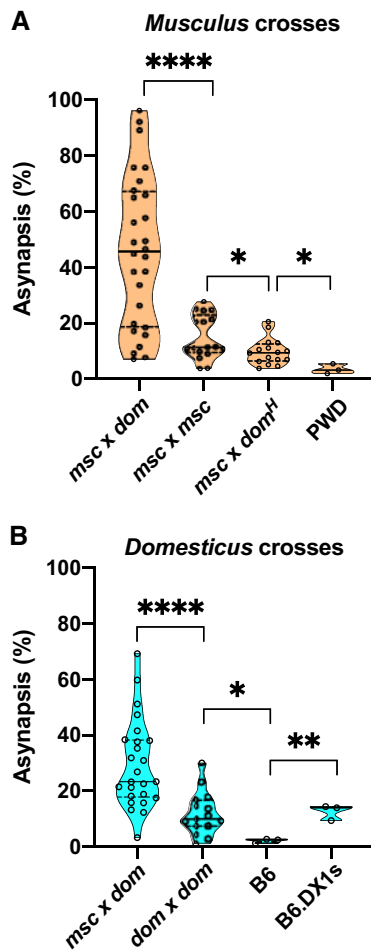


Fig. 5. Asynapsis rate in inter- and intrasubspecific crosses. (A) The overall asynapsis rate in intrasubspecific crosses of wild-derived *musculus* strains does not exceed 30%. The role of *Prdm9* in intrasubspecific crosses follows from the significant difference between *musculus* intrasubspecific and “humanized” hybrids. The lowest asynapsis rate was observed in PWD and B6 inbred strains. (B) The significant difference between inter and intrasubspecific crosses and between intrasubspecific hybrid and inbred B6 mice is apparent in *domesticus* crosses as well. Note the significant elevation of asynapsis on B6 background caused by introgression of 67-Mb of PWD sequence at the X chromosome centromeric end. Dashed lines in the violin plots denote quartiles, full line medians. *Msc*, *dom*, and *dom^H* denote *musculus*, *domesticus*, and humanized *domesticus* (*Prdm9^{dom2H}*). *P* values <0.0001****, 0.001–0.01**, 0.01–0.05*.

count between hybrids with humanized *Prdm9* allele can indicate either the presence of minor *Prdm9*-independent hybrid incompatibilities or genetically controlled physiological variations between these quantitative traits (Le Roy et al. 2001). These findings provide the first evidence for the *Prdm9* behaving as a hybrid sterility gene outside the (PWD×B6)F1 laboratory model.

Fertility Phenotypes Are Controlled by the Wild-Derived *domesticus* *Prdm9^{dom#}* Alleles

The (PWD×*domesticus*)F1 hybrids revealed varying degrees of fertility impairment estimated by the testes weight, sperm count, and meiotic asynapsis rate. The PRMD9^{dom3} ZnF array

is identical with the reference PRMD9^{dom2} of the B6 laboratory strain except for an extra copy of AVQ ZnF at position 11 (fig. 1B). After crosses with PWD females, the SIN, SIT, and SCHEST males carrying the *Prdm9^{dom3}* allele produced sterile hybrids (*Prdm9^{dom3/msc1}*, *Hstx2^{PWD}*) with sperm count close to zero and mean testes weight <80 mg. They significantly differed from other *Prdm9^{dom3}* strains, the wild-derived SPLY and laboratory strain C3H/Di (not shown), which produced fertile hybrids (see fig. 4B for statistics). Both C3H/Di and SPLY are almost entirely *domesticus* on the autosomes and X chromosome, but carry a *musculus* Y chromosome. It is unclear which modifiers in the SPLY genome ensure fertility restoration. The involvement of the Y chromosome is unlikely (see Discussion). The asynapsis estimates were unavailable for SIT and SCHEST hybrids, but the asynapsis rate of SIN and SPLY hybrids correlated with the weight of testes and the number of produced sperm (see below).

The STRB *Prdm9^{dom5}* allele also differs from the *Prdm9^{dom2}* allele only at a single ZnF repeat, in this case by deletion of the fourth ZnF at the N-terminal part of ZnF array, which is essential for the DNA-binding pattern. In accordance with the importance of the N-terminus of the array for the DNA-binding pattern, the (PWD×STRB)F1 hybrids showed physiologically normal values of sperm count (mean 32.7 million) and 27.7% asynapsis rate. The SCHUNT strain also differs by a single ZnF substitution (at position 8), in this case from *Prdm9^{dom3}*. Still, the (PWD×SCHUNT)F1 hybrids displayed the highest sperm count of 49.2 million and asynapsis rate of 21%. The most phylogenetically distant from *Prdm9^{dom2}* were *Prdm9^{dom6}* and *Prdm9^{dom7}* alleles of STAIL and STRA strains, which produced fertile hybrids with sperm counts of 42.4 and 51.4 million, respectively. They also exhibited the lowest asynapsis rates among the studied *domesticus* alleles—18.9% and 9.7%, respectively (fig. 4B).

To conclude, out of the five wild-derived *domesticus* alleles only the *Prdm9^{dom3}* allele generated sterile hybrids. The interference of genetic background was apparent from the fertility of SPLY hybrids, which carry the *Prdm9^{dom3}* allele. The SPLY differs from other *domesticus* strains (fig. 4B) by the presence of the Y chromosome of *musculus* origin, but other factor(s) in the SPLY genome can be responsible for the fertility rescue. The latter seems to be the more likely explanation as many classical laboratory strains including B6 strain also carry the *musculus* type of Y chromosome (Bishop et al. 1985; Yang et al. 2011) but produce sterile males in crosses with PWD mice.

Meiotic Asynapsis Varies within and between *Musculus* and *Domesticus* Subspecies

The most likely, though not exclusive explanation for the deficiency of proper synapsis of subspecific homeologs seems to be the asymmetry of PRDM9 binding due to differential erasure and resulting heterozygosity of PRDM9 binding motifs (Davies et al. 2016; Hinch et al. 2019). In principle, such asymmetry can vary in hybrids depending on differential erasure of the parental recombination hotspots but it drops to zero in inbred strains because of the sequence identity of homologs. To analyze *Prdm9*-related variation in meiotic

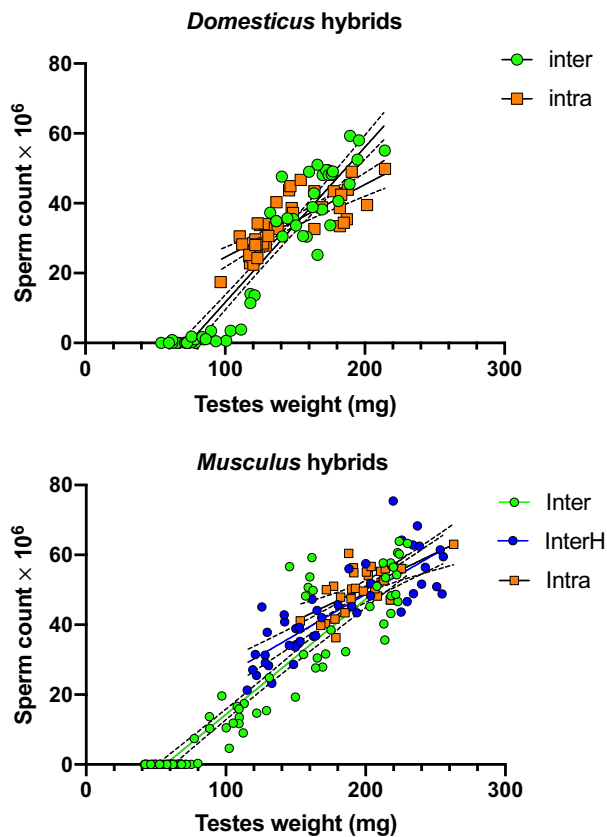


FIG. 6. Correlation between fertility phenotypes in hybrid males. Testes weight and sperm count are positively correlated in both types of hybrid males in interspecific (Pearson's $r = 0.95$, $P < 0.0001$ for *domesticus* and *musculus*), *musculus* "humanized" interspecific hybrids ($r = 0.83$, $P < 0.0001$), and intraspecific *domesticus* and *musculus* hybrids ($r = 0.78$ and 0.66 , $P < 0.0001$ for *domesticus* and *musculus*). The F1 hybrids with testes weight < 80 mg are fully sterile, producing virtually no sperm. Dashed lines denote 95% CI profile likelihood.

chromosome synapsis, we compared the overall asynapsis rates of intersubspecific hybrids (*musculus* × *domesticus*) to intrasubspecific hybrids (*domesticus* × *domesticus* and *musculus* × *musculus*) and control inbred strains (fig. 5A and B; supplementary fig. 2, Supplementary Material online) and their relation to fertility phenotypes. In intersubspecific *musculus* crosses, the asynapsis rate was reduced from median 45.7% to 9.4% by the humanized *Prdm9*^{dom2H} allele ($P < 0.0001$, Mann–Whitney test). The *musculus* intrasubspecific crosses showed median 11.3% asynapsis rate, which was significantly lower than interspecific average ($P < 0.0001$, Mann–Whitney test), but significantly higher than the asynapsis rate in the humanized crosses ($P = 0.046$, Mann–Whitney test). As predicted from the absence of hotspot asymmetry, the lowest value of asynapsis, 3.5%, was observed in the PWD strain (compared with humanized crosses $P = 0.0144$, Mann–Whitney test, fig. 5A). Similarly, in *domesticus* hybrids, the asynapsis rate was significantly higher in intersubspecific (median 23.4%) compared with the intrasubspecific hybrids (9.9%, $P < 0.0001$, Mann–Whitney test, fig. 5B), which was significantly higher than in the B6 inbred males (2.2%,

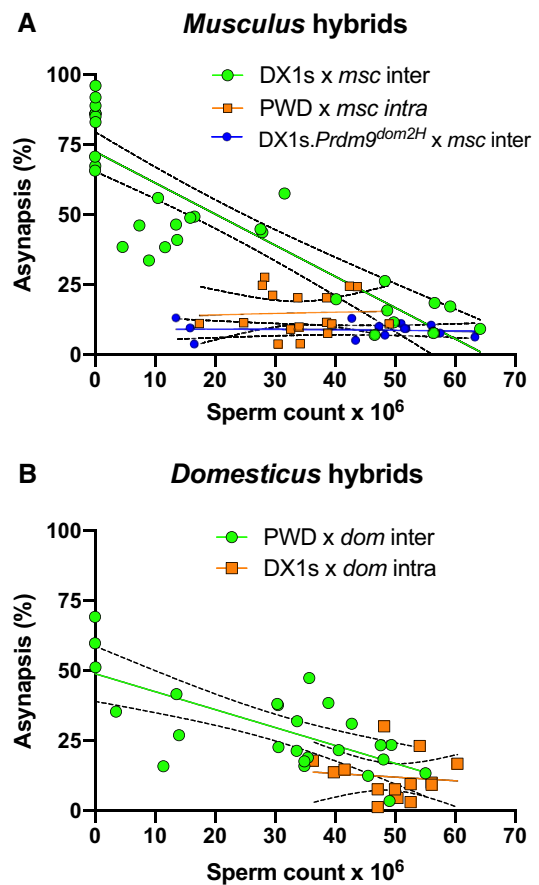


FIG. 7. Correlation between asynapsis and sperm count in hybrid males. (A) Sperm count was positively correlated only in *musculus* intersubspecific hybrids (green circles, $r = 0.87$, $P < 0.0001$) but did not show correlation in intrasubspecific (orange squares, $r = 0.05$, $P = 0.86$) and "humanized" hybrids (blue circles, $r = 0.08$, $P = 0.78$). (B) In addition, in *domesticus* crosses, only intersubspecific hybrids showed a high positive correlation between sperm count and asynapsis (green circles, $r = 0.70$, $P < 0.0001$). Dashed lines denote the first and the third quartile of the data sets.

$P = 0.0484$, unpaired *t*-test). The unexpectedly increased asynapsis rate observed in B6.DX1s compared with B6 (12.6%, $P = 0.0032$, unpaired *t*-test) cannot be explained by hotspot asymmetry and will be analyzed separately.

The sperm count and testes weight showed a positive correlation in all hybrids (fig. 6A). Testes < 80 mg produced no sperm or extremely low number of sperm cells in the epididymides and occurred exclusively in intersubspecific hybrids. Sterility was consistently associated with high asynapsis rate (range 46–96%) (fig. 7A and B; supplementary fig. S3, Supplementary Material online). In fertile intersubspecific hybrids, the asynapsis rate showed continuous variation inversely proportional to the testes weight and sperm count. Asynapsis and fertility phenotypes were not significantly correlated in intraspecific or humanized interspecific hybrids.

Discussion

The *Prdm9* gene is the first hybrid sterility gene identified in vertebrates. In this study, we investigated whether it

contributes to hybrid sterility outside the (PWD×B6)F1 laboratory hybrids where it was first described and where it has been studied until now (Forejt and Ivanyi 1974; Forejt 1996; Gregorová et al. 1996; Trachtulec et al. 1997; Mihola et al. 2009; Forejt et al. 2012; Bhattacharyya et al. 2013; Davies et al. 2016; Smagulova et al. 2016; Gregorova et al. 2018).

Variations in the Fertility of Wild-Derived Intersubspecific Hybrids Is *Prdm9* Dependent

To verify the role of various *Prdm9* alleles in hybrid sterility of mice from natural populations, we substituted one of the parents in the laboratory model of hybrid sterility with a wild-derived inbred strain from the same subspecies and compared the fertility and meiotic phenotypes of the newly derived hybrid males to that of the laboratory hybrids. Since in both experimental layouts, the genotype at a second major hybrid sterility locus was always the same (*Hstx2*^{PWD}), the differences in fertility and meiotic phenotypes between laboratory model and a newly designed hybrid could only be attributed to the introduced wild-derived *Prdm9* allele and/or additional genetic factor(s) in the wild-derived part of the genetic background (fig. 2).

In this experimental setup, the wild-derived *domesticus* males from SIN, SIT, and SCHEST strains produced infertile hybrids with PWD *musculus* females. They all shared the *domesticus Prdm9*^{dom3} allele, whose amino acid sequence is most similar to the B6 *Prdm9*^{dom2} reference “sterility” allele. The *Prdm9*^{dom3} allele was also identified in the WSB/Eij strain (Parvanov et al. 2010) derived from North American wild *domesticus* mice (Centreville, Maryland, Harr 2006, that produced quasi-sterile hybrids with PWD females, White et al. 2011). Moreover, in the same study, the QTL analysis of a (WSB×PWD)F2 population revealed an underdominant QTL locus for sperm count on proximal chromosome 17, suggesting involvement of *Prdm9*^{dom3}. Thus, altogether four wild-derived *domesticus* strains with unrelated genetic backgrounds from Germany, Scotland, and the United States carry *Prdm9*^{dom3} associated with hybrid sterility.

Admittedly, *Prdm9*^{dom3} was also found in the SPLY and C3H/Di strains, which produce fertile hybrids. Three explanations of fertility of these hybrids can be considered. First, the association of *Prdm9*^{msc1/dom3} and sterility of hybrids could be coincidental. We consider this unlikely based on the concordance of PRDM9^{dom3} ZnF variant with sterility of hybrids of four unrelated *domesticus* strains and association of PRDM9^{msc1} and PRDM9^{msc2} ZnF variants with sterility in *musculus* hybrids (fig. 4A). Second, autosomal and/or Y chromosome introgression of *musculus* genome in SPLY and C3H/Di could be responsible for restored fertility. This too seems unlikely, because SPLY and C3H were shown to carry <1% and 5% of the *musculus* autosomal genome, respectively (supplementary table S1, Supplementary Material online), an admixture too low to attenuate hybrid sterility (Gregorova et al. 2018). Likewise, the idea that presence of a *musculus*-type Y chromosome in SPLY and C3H (in contrast to other tested *domesticus* strains carrying *Prdm9*^{dom3}) (Abe et al. 2004; Morgan and Pardo-Manuel de Villena 2017) could mitigate *Prdm9*-related sterility is not supported by available evidence.

In our study (supplementary table S4, Supplementary Material online) as well as in various previous crosses, hybrid sterility clearly segregated with the *Prdm9* alleles and the X but not Y chromosome (White et al. 2011; Campbell et al. 2012; Dzur-Gejdosova et al. 2012; Bhattacharyya et al. 2013; Gregorova et al. 2018). The X–Y intragenomic conflict caused by the copy-number imbalance of the *Slx/Slx1* and *Sly* gene families in hybrids does lead to a hybrid sterility-like incompatibility (Cocquet et al. 2009, 2012; Campbell et al. 2012). However, *Prdm9*-related infertility operates at the first meiotic prophase, upstream of the postmeiotic defects associated with X–Y intragenomic conflict. Notwithstanding, it is highly likely that the X–Y conflict can operate as a hybrid sterility barrier independently of *Prdm9*, and, in the case of partial *Prdm9*-controlled hybrid fertility with attenuated early meiotic arrest, the X–Y interactions could contribute to the strength of the overall reproductive barrier between subspecies (Martincová et al. 2019). The third explanation seems most likely so far. The renewed fertility of *Prdm9*^{dom3} hybrids could be either a consequence of presumed low level of erosion of PRDM9^{dom3} binding sites in SPLY and C3H strains, or due to action of polymorphic accessory factors promoting PRDM9 binding (Mahgoub et al. 2020; Spruce et al. 2020).

Hybrid male sterility was also observed in *musculus* wild-derived hybrids, where it was restricted to the *Prdm9*^{msc1} allele (STUS and PWD strains) and closely similar *Prdm9*^{msc2} (SKE) allele. To distinguish the effect of *Prdm9* gene from unrelated hybrid sterility factor(s) in the genetic background, we substituted the *domesticus Prdm9*^{dom2} of the B6.DX1s parent with humanized *Prdm9*^{dom2H} carrying the ZnF array from the human PRDM9^B variant. Because the human PRDM9 binding sites have no history of evolutionary erasure in the naïve mouse genome, *Prdm9*^{dom2H} is thought to reverse sterility of (PWD×B6. *Prdm9*^{dom2H})F1 hybrids by reducing PRDM9 hotspot asymmetry (Davies et al. 2016). Consequently, if the *Prdm9*-dependent erasure of DSB hotspots is the main cause of fertility impairment of B6.DX1s×*musculus* hybrids, we can expect the humanized allele to improve their fertility phenotypes. Indeed, as expected, the humanized *Prdm9*^{dom2H} gene significantly increased the testes weight, number of sperm, and normalized meiotic chromosome synapsis in intersubspecific hybrids, thus confirming the absence of a major *Prdm9*-unrelated mechanism of male sterility.

Variation of Meiotic Synapsis and Fertility Parameters within Subspecies

We found that meiotic asynapsis rate >60% is diagnostic for full hybrid sterility in *musculus* and *domesticus* intersubspecific F1 hybrids. Remarkably, variation of asynapsis was also found in intrasubspecific crosses within the range of 1.2–30% in intra-*domesticus* hybrids and 3.8–27.6% in intra-*musculus* hybrids. It is tempting to speculate that the increased levels of asynapsis in intrasubspecific crosses represent a cytological counterpart of hotspot asymmetry between populations within the same subspecies. To verify the idea, direct estimation of the DSB hotspot asymmetry in intraspecific F1 hybrids and their parental strains are necessary.

Prdm9-Dependent Hybrid Sterility in *Musculus/Domesticus* Hybrid Zone?

Our relatively simple model of hybrid sterility composed of *Prdm9*, *Hstx2*, and genomic asymmetry of PRDM9 binding sites contrasts with the complex polygenic control found in wild mice from the European hybrid zone or from the laboratory intercrosses between wild-derived inbred strains. We believe that the difference can be explained by multiplicity of unrelated reproductive isolation mechanisms differentially revealed by different experimental approaches. For instance, the studies of gene flow across the hybrid zone (Tucker et al. 1992; Macholan et al. 2007; Teeter et al. 2007, 2010; Janoušek et al. 2012) can reveal regions in the genome that are resistant to introgression and potentially carry genes affecting any form of reproductive fitness at prezygotic and/or postzygotic level. In addition, the genome-wide association studies of male fertility in two feline interspecies models (Davis et al. 2015) and in mice from the hybrid zone (Turner and Harr 2014) disclosed complex genetic networks potentially affecting unrelated phenotypes of reproductive isolation. The mouse study included strong GWAS interactions between loci on Chromosomes X and 17, which, however, clearly mapped outside the *Prdm9* and *Hstx2* loci. The *Prdm9*-dependent hybrid sterility requires F1 hybrid genetic background since even small stretches of consubspecific sequence present in multiple chromosomes can rescue meiotic synapsis and fertility of hybrids (Gregorova et al. 2018).

The laboratory crosses of wild-derived mouse strains designed to map fertility phenotypes (Good et al. 2007; Vyskocilova et al. 2009; Oka et al. 2010; White et al. 2011, 2012; Wang et al. 2015; Larson et al. 2018; Schwahn et al. 2018) or gene misexpression in hybrid testis (Mack et al. 2016; Mack and Nachman 2017; Morgan et al. 2020) are much closer to our F1 hybrid sterility model. However, although the classical F1 hybrid sterility is governed by underdominance, the fertility of intersubspecific backcrosses and F2 crosses is affected by more frequent autosomal recessive incompatibilities (Coyne and Orr 2004; White et al. 2011). Indeed, in a study of (PWD×WSB)F2 hybrid population (White et al. 2011), out of 19 autosomal QTLs only three were underdominant, two of them for sperm density and testes size on chromosome 17. Admittedly, there must be some additional genetic factors in *Prdm9*-controlled hybrid sterility, besides *Prdm9*, *Hstx2*, and background heterozygosity, that modify fertility of F1 hybrids. The hybrid sterility factors on chromosomes 3, 9, and 13 polymorphic between PWD and STUS *musculus* strains could represent possible examples (Bhattacharyya et al. 2014).

Previously, it was shown that the intersubspecific F1 hybrids are virtually missing in the central parts of the European zone so that a pure form of F1 hybrid sterility, as seen in (PWD×B6) laboratory crosses, could hardly function as a major reproductive barrier (Macholan et al. 2007; Teeter et al. 2010; Albrechtova et al. 2012; Turner et al. 2012). On the other hand, we know that the *Prdm9*-dependent meiotic arrest and associated asynapsis between homeologous autosomes gradually weakens, but does not disappear in intersubspecific laboratory backcrosses (Dzur-Gejdosova et al. 2012;

Gregorova et al. 2018). We can speculate that similar intersubspecific and consubspecific genomic mixture reduces the *Prdm9* hotspot asymmetry and results in the prevalence of recessive incompatibilities within the hybrid zone. Future studies will be necessary to elucidate the role of the *Prdm9*-controlled hybrid sterility in maintenance of the current hybrid zone between the *musculus* and *domesticus* subspecies of house mouse.

To conclude, our data show for the first time that the male infertility of wild-derived *musculus* and *domesticus* subspecies F1 hybrids is controlled by *Prdm9* as the major hybrid sterility gene. The impaired fertility surrogates, testes weight and sperm count, negatively correlated with increasing difficulties of meiotic synapsis of homologous chromosomes and meiotic arrest, which might reflect the increasing asymmetry of PRDM9-dependent DNA DSBs.

Materials and Methods

Mice

Except for the PWD/Ph strain (Gregorova and Forejt 2000), all wild-derived inbred strains (F13–F61) in this study have been developed and maintained in the breeding facility of the Institute of Vertebrate Biology in Studenec (Pialek et al. 2007; Baird and Macholan 2012; Albrechtová et al. 2014; Martinová et al. 2019), with licenses for maintaining the mice and experimental work (61,974/2017-MZE-17214 and 62,065/2017-MZE-17214, respectively). The localities of origin of the *musculus* strains are: SKA/Jpia—Kaerepere, Estonia, [N: 58° 57', E: 24° 50'], SKE/Jpia—Keava, Estonia [N: 58° 56' 27'', E: 24° 54'], BULS/Jpia and BUSNA/Jpia—Buškovice, Czech Republic [N: 50° 13', E: 13° 23'], PWD/Ph—Kunratice (Prague), Czech Republic, STUF/Jpia and STUS/Jpia—Studenec, Czech Republic [N: 49° 12', E: 16° 04'], SENK/Jpia—Šenkvice, Slovak Republic [N: 48° 18', E: 17° 21']. The *domesticus* strains: STRA/Jpia and STRB/Jpia—Straas, Bavaria, Germany [N: 50° 11', E: 11° 46'], STAIL/Jpia, SCHEST/Jpia and SCHUNT/Jpia—Schweben, Hessen, Germany [N: 50° 26', E: 9° 35'], SPLY/Jpia—Plössen, Bavaria, Germany [N: 49° 51' 18'', E: 11° 47'], SIN/Jpia and SIT/Jpia—Scar, Whitemill Bay, Sanday Island, Orkneys, Scotland [N: 59° 18', E: −2° 33'].

The C57BL/6j-Chr X.1s^{PWD/Ph}/Forej (in short, B6.DX1s) is a consomic strain carrying 69.6 Mb of the proximal PWD sequence on the genetic background of the B6/J strain (Bhattacharyya et al. 2014). Coisogenic strain C57BL/6-*Prdm9*^{TmHu} (abbreviated B6.*Prdm9*^{dom2H}) (Davies et al. 2016) was kindly provided by Dr Simon Myers, Oxford University, UK. All mice were maintained in the Specific Pathogen-Free Facilities, in accordance to animal care protocols approved by the Committee on the Ethics of Animal Experiments of the Institute (No. 141/2012). The animal care obeyed the Czech Republic Act for Experimental Work with Animals (Decree No. 207/2004 Sb and Acts Nos 246/92 Sb and 77/2004 Sb), fully compatible with the corresponding regulations and standards of the European Union (Council Directive 86/609/EEC and Appendix A of the Council of Europe Convention ETS123).

Genotyping of Mouse Strains and Quality Control

One male and one female from each of 17 strains of interest (including PWK/Ph and C57BL/6j) were genotyped at 143,259 markers with the GigaMUGA array (Neogen Europe, Ayr, Scotland). An updated annotation for the GigaMUGA array (https://kbroman.org/MUGAarrays/new_annotations.html; last accessed July 11, 2020) was used for all subsequent analyses. All samples had <10% missing calls, a useful cutoff for this platform (Morgan et al. 2015), and <5% heterozygous calls, as expected for inbred strains. The sex of each sample was confirmed by comparing hybridization intensities for X- and Y-linked markers.

Ancestry Inference

To define ancestry-informative markers, we used published genotypes on the GigaMUGA array from 15 wild-caught *M. m. domesticus* and 5 wild-caught *M. m. musculus* individuals (Morgan 2015). The *domesticus* set includes mice trapped in Greece, Spain, Italy, Switzerland, and the eastern United States. The *musculus* set includes mice trapped in China, Poland, Germany, and Russia. All trapping locations were far from the *musculus*–*domesticus* hybrid zone, so these individuals are presumed to be pure representatives of their subspecies.

Autosomes and X Chromosome. Markers with absolute allele frequency difference >0.75 between the *musculus* and *domesticus* reference groups and <25% missing genotypes within each group were retained as putative ancestry-informative sites. A total of 28,146 unique autosomal and 1,303 X-linked sites were retained. Genotypes for inbred strains of interest were recoded as *musculus*, *domesticus*, or heterozygous at each marker according to the consensus allele in each reference group. A hidden Markov model (HMM) was then used to decode ancestry along the genome of each inbred strain. The HMM has two hidden states, *musculus* and *domesticus*. (Given the low observed residual heterozygosity in these strains, a *musculus*/*domesticus* heterozygous state was not modeled.) The probability of transition between states between consecutive sites is $1e^{-5}$; the probability of observing the opposite subspecies' allele is $5e^{-2}$; and probability of observing a heterozygous genotype is $1e^{-3}$. Although these parameters were set arbitrarily, we confirmed that the output of the procedure is relatively insensitive to their values. The HMM was applied separately to observed genotypes of each sample, and the posterior decoding was obtained by the Viterbi algorithm. Per-site ancestry was aggregated into blocks by simple run-length encoding. For strains previously analyzed using the Mouse Diversity Array (Yang et al. 2011), we confirmed by manual inspection that introgressed blocks >5 Mb in size were recovered in both platforms. Analyses were performed in “R” v3.3.2 using packages “argyle” (<https://github.com/andrewparkermorgan/argyle>; last accessed July 11, 2020) and “HMM” (<https://cran.r-project.org/package=HMM>; last accessed July 11, 2020). The ancestry origin of C3H/Di strain was extrapolated from Mouse Phylogeny Viewer (<http://msub.csbio.unc.edu/>; last accessed July 11, 2020).

Sequencing of Mouse *Prdm9* Alleles and Phylogeny

Partially purified DNA from mouse spleens was isolated by Puregene Core Kit A (QIAGEN 158267) according to the manufacturer's instructions. DNA template of 50–100 ng was used for amplification of *Prdm9* Exon12 in a reaction mixture containing primers for *Prdm9* Exon12: Exon12-L1—TGAGATCTGAGGAAAGTAAGAG and Exon12-R—TGCTGTTGGCTTTCATTC with a concentration of 0.4 μ M of each primer, 0.2 mM dNTP, 2 mM MgCl₂, and Taq DNA Polymerase, recombinant (1 U/ml) (ThermoFisher Scientific EP0404) by 0.15 U per reaction. Samples were amplified by BIOER XP Cycler under the PCR program: 94 °C for 5 min and 40 cycles at 94 °C for 30 s, 61 °C for 1 min, 68 °C for 2 min, and a single step after the cycles of 72 °C for 7 min. The PCR products were resolved in 2% agarose gel allowing visual estimation of the quality and homogeneity of amplified DNA. The samples were prepared for sequencing as ExoSAP-treated samples. The obtained sequencing data were visualized and extracted by the Chromas Lite 2.1 application.

In crosses between heterozygous *Prdm9*^{dom2H/+} females versus wild males, the type of *Prdm9* allele in the hybrid offspring was checked by forward primer (5'-TTCTGCCATCACTTCCTCGGTGA-3') and reverse primer (5'-TCTGAAGCCCACTATTTCAATACCCC-3'). A 677-bp amplicon was obtained from the humanized allele and a 491-bp amplicon was obtained from the wild-type allele (Davies et al. 2016). The reaction mixture was the same as for the sequencing of *Prdm9* Exon12 by PCR program: 95 °C for 2 min and 40 cycles at 95 °C for 30 s, 55 °C for 40 s, 72 °C for 40 s, and a single step after the cycles of 72 °C for 3 min.

The evolutionary relationships of among *Prdm9* alleles were inferred using the neighbor-joining method (Saitou and Nei 1987). The optimal tree with the sum of branch length = 0.03369633 is shown. The percentage of replicate trees in which the associated taxa clustered together in the bootstrap test (10,000 replicates) is shown next to the branches (Felsenstein 1985). The tree is drawn to scale, with branch lengths in the same units as those of the evolutionary distances used to infer the phylogenetic tree. The evolutionary distances were computed using the maximum composite likelihood method (Tamura et al. 2004) and are in the units of the number of base substitutions per site. This analysis involved 17 nucleotide sequences. Codon positions included were 1st + 2nd + 3rd + Noncoding. All ambiguous positions were removed for each sequence pair (pairwise deletion option). There were a total of 1,263 positions in the final data set. Evolutionary analyses were conducted in MEGA X (Kumar et al. 2018).

Fertility Phenotyping

Males were euthanized by cervical dislocation at 60 dpp and their body weight, the weight of paired testes in milligrams (TW), and sperm count in million was determined. Since the correlation between the body weight and testes weight was not significant in hybrid males (supplementary fig. S4, Supplementary Material online), we used the absolute weight of paired testes as one of the fertility phenotypes. Spermatozoa were released from the whole epididymides,

and the number of sperm heads was counted in 25 squares of a Bürker chamber using an Olympus CX41 microscope under 200× magnification (for details, see Vyskočilová et al. [2005]). For each F1 cross, four to eight hybrid males were examined for testes weight and sperm count.

Immunostaining and Asynapsis Rate Determination

For immunocytochemistry, the spread spermatocyte nuclei were prepared as described (Anderson et al. 1999) with modifications. Briefly, a single-cell suspension of spermatogenic cells in 0.1 M sucrose with protease inhibitors (Roche) was dropped on 1% paraformaldehyde-treated slides and allowed to settle for 3 h in a humidified box at 4 °C. After brief washing in distilled water and PBS and blocking with 5% goat sera in PBS (vol/vol), the cells were immunolabeled using a standard protocol with the following antibodies: anti-HORMAD2 (1:700, rabbit polyclonal antibody, a gift from Attila Toth) and SYCP3 (1:100, mouse monoclonal antibody, Santa Cruz, #74569). Centromere painting was done by human antibodies from autoimmune serum, AB-Incorporated, 15-235. Rabbit α - γ -H2AX (1:1,000, Rabbit polyclonal anti gamma H2AX, ABCAM, ab2893) identified early DSBs and unsynapsed parts of autosomes and sex chromosomes. Secondary antibodies were used at 1:300 dilutions and incubated at 4 °C for 60 min: goat anti-Mouse IgG-AlexaFluor568 (MolecularProbes, A-11031), goat anti-Rabbit IgG-AlexaFluor647 (MolecularProbes, A-21245), goat anti-Human IgG-AlexaFluor647 (MolecularProbes, A-21445), goat anti-Rabbit IgG-AlexaFluor488 (MolecularProbes, A-11034).

The images were acquired and examined using a Nikon Eclipse 400 microscope with a motorized stage control using a Plan Fluor objective, 60× (MRH00601; Nikon) and captured using a DS-QiMc monochrome CCD camera (Nikon) and the NIS-Elements program (Nikon). The images were processed using the Image J software (Schneider et al. 2012). For each sample, we analyzed between 68 and 121 pachynemas. The number of asynapses per nucleus was scored in each pachynema. One asynapsis was equal to one HORMAD2 stained element, excluding XY chromosomes. The asynapsis rate was represented as the percentage of pachynemas with asynapses out of the total number of the checked pachynemas of each male. A minimum of three males per F1 cross was used for asynapsis rate estimation.

Statistics

The statistical significance for the testes weight and sperm count was assessed by two-tailed Mann–Whitney test. Asynapsis rate was evaluated by unpaired *t*-test in the GraphPad Prism version 8.4.0. for MacOS.

Supplementary Material

Supplementary data are available at *Molecular Biology and Evolution* online.

Acknowledgments

We thank Simon Myers for the B6.Prdm9^{dom2H} mice, Attila Toth for HORMAD2 antibody, and Sarka Takacova for

comments. This work was funded by LQ1604 Project of the National Sustainability Program II from the Ministry of Education, Youth and Sports of the Czech Republic, and by Czech Science Foundation (Grant Nos. GA CR No. 17-04364S to E.P., 20-04075S to J.F., and 19-12774S to J.P.).

References

- Abe K, Noguchi H, Tagawa K, Yuzuriha M, Toyoda A, Kojima T, Ezawa K, Saitou N, Hattori M, Sakaki Y, et al. 2004. Contribution of Asian mouse subspecies *Mus musculus molossinus* to genomic constitution of strain C57BL/6j, as defined by BAC-end sequence-SNP analysis. *Genome Res.* 14(12):2439–2447.
- Albrechtová J, Albrecht T, Baird SJ, Macholan M, Rudolfson G, Munclinger P, Tucker PK, Pialek J. 2012. Sperm-related phenotypes implicated in both maintenance and breakdown of a natural species barrier in the house mouse. *Proc R Soc B.* 279(1748):4803–4810.
- Albrechtová J, Albrecht T, Dureje L, Pallazola VA, Pialek J. 2014. Sperm morphology in two house mouse subspecies: do wild-derived strains and wild mice tell the same story? *PLoS One* 9(12):e115669.
- Anderson LK, Reeves A, Webb LM, Ashley T. 1999. Distribution of crossing over on mouse synaptonemal complexes using immunofluorescent localization of MLH1 protein. *Genetics* 151:1569.
- Baird SJE, Macholan M. 2012. What can the *Mus musculus musculus*/*M. m. domesticus* hybrid zone tell us about speciation? In: Macholan M, Baird SJ, Muclinger P, Pialek J, editors. Evolution of the house mouse. Cambridge: Cambridge University Press. p. 334–372.
- Baker CL, Kajita S, Walker M, Saxl RL, Raghupathy N, Choi K, Petkov PM, Paigen K. 2015. PRDM9 drives evolutionary erosion of hotspots in *Mus musculus* through haplotype-specific initiation of meiotic recombination. *PLoS Genet.* 11(1):e1004916.
- Baker CL, Walker M, Kajita S, Petkov PM, Paigen K. 2014. PRDM9 binding organizes hotspot nucleosomes and limits Holliday junction migration. *Genome Res.* 24(5):724–732.
- Barbash DA, Siino DF, Tarone AM, Roote J. 2003. A rapidly evolving MYB-related protein causes species isolation in *Drosophila*. *Proc Natl Acad Sci U S A.* 100(9):5302–5307.
- Baudat F, Buard J, Grey C, Fledel-Alon A, Ober C, Przeworski M, Coop G, de Massy B. 2010. PRDM9 is a major determinant of meiotic recombination hotspots in humans and mice. *Science* 327(5967):836–840.
- Bhattacharyya T, Gregorova S, Mihola O, Anger M, Sebestova J, Denny P, Simecek P, Forejt J. 2013. Mechanistic basis of infertility of mouse intersubspecific hybrids. *Proc Natl Acad Sci U S A.* 110(6):E468–E477.
- Bhattacharyya T, Reifova R, Gregorova S, Simecek P, Gergelits V, Mistrik M, Martinova I, Pialek J, Forejt J. 2014. X chromosome control of meiotic chromosome synapsis in mouse inter-subspecific hybrids. *PLoS Genet.* 10(2):e1004088.
- Bishop CE, Boursot P, Baron B, Bonhomme F, Hatat D. 1985. Most classical *Mus musculus domesticus* laboratory mouse strains carry a *Mus musculus musculus* Y chromosome. *Nature* 315(6014):70–72.
- Boulton A, Myers RS, Redfield RJ. 1997. The hotspot conversion paradox and the evolution of meiotic recombination. *Proc Natl Acad Sci U S A.* 94(15):8058–8063.
- Boursot P, Din W, Anand R, Darviche D, Dod B, Von Deimling F, Talwar GP, Bonhomme F. 1996. Origin and radiation of the house mouse: mitochondrial DNA phylogeny. *J Evol Biol.* 9(4):391–415.
- Buard J, Rivals E, Dunoyer de Segonzac D, Garres C, Caminade P, de Massy B, Boursot P. 2014. Diversity of Prdm9 zinc finger array in wild mice unravels new facets of the evolutionary turnover of this coding minisatellite. *PLoS One* 9(1):e85021.
- Campbell P, Good JM, Dean MD, Tucker PK, Nachman MW. 2012. The contribution of the Y chromosome to hybrid male sterility in house mice. *Genetics* 191(4):1271–1281.
- Cocquet J, Ellis PJ, Mahadevaiah SK, Affara NA, Vaiman D, Burgoyne PS. 2012. A genetic basis for a postmeiotic X versus Y chromosome intragenomic conflict in the mouse. *PLoS Genet.* 8(9):e1002900.
- Cocquet J, Ellis PJ, Yamauchi Y, Mahadevaiah SK, Affara NA, Ward MA, Burgoyne PS. 2009. The multicopy gene *Sly* represses the sex

- chromosomes in the male mouse germline after meiosis. *PLoS Biol.* 7(11):e1000244.
- Coyne JA, Orr HA. 2004. Speciation. Sunderland (MA): Sinauer Associates.
- Darwin C. 1859. On the origin of species by means of natural selection or the preservation of favored races in the struggle for life. London: Murray.
- Davies B, Hatton E, Altemose N, Hussin JG, Pratto F, Zhang G, Hinch AG, Moralli D, Biggs D, Diaz R, et al. 2016. Re-engineering the zinc fingers of PRDM9 reverses hybrid sterility in mice. *Nature* 530(7589):171–176.
- Davis BW, Seabury CM, Brashear WA, Li G, Roelke-Parker M, Murphy WJ. 2015. Mechanisms underlying mammalian hybrid sterility in two feline interspecies models. *Mol Biol Evol.* 32(10):2534–2546.
- Dion-Cote AM, Barbash DA. 2017. Beyond speciation genes: an overview of genome stability in evolution and speciation. *Curr Opin Genet Dev.* 47:17–23.
- Dobzhansky T. 1951. Genetics and the origin of species. New York: Columbia University.
- Dobzhansky T. 1936. Studies on hybrid sterility. II. Localization of sterility factors in *Drosophila pseudoobscura* hybrids. *Genetics* 21(2):113–135.
- Dufkova P, Macholan M, Pialek J. 2011. Inference of selection and stochastic effects in the house mouse hybrid zone. *Evolution* 65:993–1010.
- Dureje L, Macholan M, Baird SJE, Pialek J. 2012. The mouse hybrid zone in Central Europe: from morphology to molecules. *Folia Zool.* 61(3–4):308–318.
- Duvaux L, Belkhir K, Boulesteix M, Boursot P. 2011. Isolation and gene flow: inferring the speciation history of European house mice. *Mol Ecol.* 20(24):5248–5264.
- Dzur-Gejdosova M, Simecek P, Gregorova S, Bhattacharyya T, Forejt J. 2012. Dissecting the genetic architecture of F1 hybrid sterility in house mice. *Evolution* 66(11):3321–3335.
- Eram MS, Bustos SP, Lima-Fernandes E, Siarheyeva A, Senisterra G, Hajian T, Chau I, Duan S, Wu H, Dombrovski L, et al. 2014. Trimethylation of histone H3 lysine 36 by human methyltransferase PRDM9 protein. *J Biol Chem.* 289(17):12177–12188.
- Felsenstein J. 1985. Confidence limits on phylogenies: an approach using the bootstrap. *Evolution* 39(4):783–791.
- Forejt J. 1996. Hybrid sterility in the mouse. *Trends Genet.* 12(10):412–417.
- Forejt J. 1984. X-inactivation and its role in male sterility. In: Bennett M, Gropp A, Wolf U, editors. Chromosomes today. London: George Allen and Unwin. p. 117–127.
- Forejt J, Ivanyi P. 1974. Genetic studies on male sterility of hybrids between laboratory and wild mice (*Mus musculus* L.). *Genet Res.* 24(2):189–206.
- Forejt J, Pialek J, Trachtulec Z. 2012. Hybrid male sterility genes in the mouse subspecific crosses. In: Macholan M, Baird SJE, Muclinger P, Pialek J, editors. Evolution of the house mouse. Cambridge: Cambridge University Press. p. 482–503.
- Geraldes A, Basset P, Gibson B, Smith KL, Harr B, Yu HT, Bulatova N, Ziv Y, Nachman MW. 2008. Inferring the history of speciation in house mice from autosomal, X-linked, Y-linked and mitochondrial genes. *Mol Ecol.* 17(24):5349–5363.
- Gergelits V, Parvanov E, Simecek P, Forejt J. 2019. Chromosome-wide distribution and characterization of interspecific meiotic non-crossovers in mice. bioRxiv. 792226.
- Good JM, Dean MD, Nachman MW. 2008. A complex genetic basis to X-linked hybrid male sterility between two species of house mice. *Genetics* 179(4):2213–2228.
- Good JM, Handel MA, Nachman MW. 2007. Asymmetry and polymorphism of hybrid male sterility during the early stages of speciation in house mice. *Evol Int J Org Evol.* 62:50–65.
- Gregorova S, Forejt J. 2000. PWD/Ph and PWK/Ph inbred mouse strains of *Mus m. musculus* subspecies – a valuable resource of phenotypic variations and genomic polymorphisms. *Folia Biol (Praha).* 46:31–41.
- Gregorova S, Gergelits V, Chvatalova I, Bhattacharyya T, Valiskova B, Fotopulosova V, Jansa P, Wiatrowska D, Forejt J. 2018. Modulation of Prdm9-controlled meiotic chromosome asynapsis overrides hybrid sterility in mice. *Elife* 7:pil e34282.
- Gregorová S, Mňuková-Fajdelová M, Trachtulec Z, Čapkova J, Loudová M, Høglund M, Hamvas R, Lehrach H, Vínček V, Klein J, et al. 1996. Sub-millimorgan map of the proximal part of mouse chromosome 17 including the hybrid sterility 1 gene. *Mamm Genome.* 7(2):107–113.
- Haldane J. 1922. Sex ration and unisexual sterility in animal hybrids. *J Gen.* 12(2):101–109.
- Harr B. 2006. Genomic islands of differentiation between house mouse subspecies. *Genome Res.* 16(6):730–737.
- Hayashi K, Matsui Y. 2006. Meisetz, a novel histone tri-methyltransferase, regulates meiosis-specific epigenesis. *Cell Cycle* 5(6):615–620.
- Hinch AG, Zhang G, Becker PW, Moralli D, Hinch R, Davies B, Bowden R, Donnelly P. 2019. Factors influencing meiotic recombination revealed by whole-genome sequencing of single sperm. *Science* 363(6433):eaau8861.
- Hunter N. 2015. Meiotic recombination: the essence of heredity. *Cold Spring Harb Perspect Biol.* 7:a016618.
- Janoušek V, Wang L, Luzynski KEN, Dufková P, Vyskočilová MM, Nachman MW, Munclinger P, Macholan M, Pialek J, Tucker PK. 2012. Genome-wide architecture of reproductive isolation in a naturally occurring hybrid zone between *Mus musculus musculus* and *M. m. domesticus*. *Mol Ecol.* 21(12):3032–3047.
- Kono H, Tamura M, Osada N, Suzuki H, Abe K, Moriwaki K, Ohta K, Shiroishi T. 2014. Prdm9 polymorphism unveils mouse evolutionary tracks. *DNA Res.* 21(3):315–326.
- Kumar S, Stecher G, Li M, Knyaz C, Tamura K. 2018. MEGA X: molecular evolutionary genetics analysis across computing platforms. *Mol Biol Evol.* 35(6):1547–1549.
- Larson EL, Vanderpool D, Sarver BAJ, Callahan C, Keeble S, Provencio LL, Kessler MD, Stewart V, Nordquist E, Dean MD, et al. 2018. The evolution of polymorphic hybrid incompatibilities in house mice. *Genetics* 209(3):845–859.
- Le Roy I, Tordjman S, Migliore-Samour D, Degrelle H, Roubertoux PL. 2001. Genetic architecture of testis and seminal vesicle weights in mice. *Genetics* 158(1):333–340.
- Lustyk D, Kinsky S, Ullrich KK, Yancoskie M, Kasikova L, Gergelits V, Sedlacek R, Chan YF, Odenthal-Hesse L, Forejt J, et al. 2019. Genomic structure of Hstx2 modifier of Prdm9-dependent hybrid male sterility in mice. *Genetics* 213(3):1047–1063.
- Mack KL, Campbell P, Nachman MW. 2016. Gene regulation and speciation in house mice. *Genome Res.* 26(4):451–461.
- Mack KL, Nachman MW. 2017. Gene regulation and speciation. *Trends Genet.* 33(1):68–80.
- Maheshwari S, Barbash DA. 2011. The genetics of hybrid incompatibilities. *Annu Rev Genet.* 45(1):331–355.
- Mahgoub M, Paiano J, Bruno M, Wu W, Pathuri S, Zhang X, Ralls S, Cheng X, Nussenzweig A, Macfarlan TS. 2020. Dual histone methyl reader ZCWPW1 facilitates repair of meiotic double strand breaks in male mice. *Elife* 9:e53360.
- Macholan M, Baird SJ, Dufkova P, Munclinger P, Bimova BV, Pialek J. 2011. Assessing multilocus introgression patterns: a case study on the mouse X chromosome in central Europe. *Evolution* 65(5):1428–1446.
- Macholan M, Baird SJE, Fornuskova A, Martincova I, Rubik P, Dureje L, Heitlinger E, Pialek J. 2019. Widespread introgression of the *Mus musculus musculus* Y chromosome in Central Europe. *bioRxiv* 12.23.887471.
- Macholan M, Munclinger P, Sugerkova M, Dufkova P, Bimova B, Bozikova E, Zima J, Pialek J. 2007. Genetic analysis of autosomal and X-linked markers across a mouse hybrid zone. *Evolution* 61(4):746–771.
- Macholan M, Vyskočilová M, Bonhomme F, Kryštufek B, Orth A, Vohralík V. 2007. Genetic variation and phylogeography of free-living mouse species (genus *Mus*) in the Balkans and the Middle East. *Mol Ecol.* 16(22):4774–4788.
- Martincová I, Dureje L, Kreisinger J, Macholan M, Pialek J. 2019. Phenotypic effects of the Y chromosome are variable and structured

- in hybrids among house mouse recombinant lines. *Ecol Evol.* 9(10):6124–6137.
- Masly JP, Jones CD, Noor MA, Locke J, Orr HA. 2006. Gene transposition as a cause of hybrid sterility in *Drosophila*. *Science* 313(5792):1448–1450.
- Mayr E. 1963. Animal species and evolution. Cambridge: Harvard University Press.
- Mihola O, Pratto F, Brick K, Linhartova E, Kobets T, Flachs P, Baker CL, Sedlacek R, Paigen K, Petkov PM, et al. 2019. Histone methyltransferase PRDM9 is not essential for meiosis in male mice. *Genome Res.* 29(7):1078–1086.
- Mihola O, Trachtulec Z, Vlcek C, Schimenti JC, Forejt J. 2009. A mouse speciation gene encodes a meiotic histone H3 methyltransferase. *Science* 323(5912):373–375.
- Morgan AP. 2015. argyle: an R package for analysis of Illumina genotyping arrays. *G3 (Bethesda)* 6:281–286.
- Morgan AP, Fu CP, Kao CY, Welsh CE, Didion JP, Yadgary L, Hyacinth L, Ferris MT, Bell TA, Miller DR. 2015. The Mouse Universal Genotyping Array: from substrains to subspecies. *G3 (Bethesda)* 6:263–279.
- Morgan AP, Pardo-Manuel de Villena F. 2017. Sequence and structural diversity of mouse Y chromosomes. *Mol Biol Evol.* 34(12):3186–3204.
- Morgan K, Harr B, White MA, Payseur BA, Turner LM. 2020. Disrupted gene networks in subfertile hybrid house mice. *Mol Biol Evol.* 37(6):1547–1562.
- Muller H, Pontecorvo G. 1942. Recessive genes causing interspecific sterility and other disharmonies between *Drosophila melanogaster* and *simulans*. *Genetics.* 27:157.
- Muller HJ. 1942. Isolation mechanisms, evolution and temperature. *Biol Symp.* 6:71–125.
- Myers S, Bowden R, Tumian A, Bontrop RE, Freeman C, MacFie TS, McVean G, Donnelly P. 2010. Drive against hotspot motifs in primates implicates the PRDM9 gene in meiotic recombination. *Science* 327(5967):876–879.
- Nagamine CM, Nishioka Y, Moriwaki K, Boursot P, Bonhomme F, Lau YF. 1992. The musculus-type Y chromosome of the laboratory mouse is of Asian origin. *Mamm Genome.* 3(2):84–91.
- Naveira H, Maside X. 1998. The genetics of hybrid male sterility in *Drosophila*. In: Howard D, Berlocher S, editors. Endless forms. Oxford: Oxford University. p. 330–338.
- Oka A, Mita A, Takada Y, Koseki H, Shiroishi T. 2010. Reproductive isolation in hybrid mice due to spermatogenesis defects at three meiotic stages. *Genetics* 186(1):339–351.
- Oliver PL, Goodstadt L, Bayes JJ, Birtle Z, Roach KC, Phadnis N, Beatson SA, Lunter G, Malik HS, Ponting CP. 2009. Accelerated evolution of the Prdm9 speciation gene across diverse metazoan taxa. *PLoS Genet.* 5(12):e1000753.
- Paigen K, Petkov PM. 2018. PRDM9 and its role in genetic recombination. *Trends Genet.* 34(4):291–300.
- Parvanov ED, Petkov PM, Paigen K. 2010. Prdm9 controls activation of mammalian recombination hotspots. *Science* 327(5967):835–835.
- Payseur BA, Krenz JG, Nachman MW. 2004. Differential patterns of introgression across the X chromosome in a hybrid zone between two species of house mice. *Evolution* 58(9):2064–2078.
- Payseur BA, Presgraves DC, Filatov DA. 2018. Introduction: sex chromosomes and speciation. *Mol Ecol.* 27(19):3745–3748.
- Phadnis N, Orr HA. 2009. A single gene causes both male sterility and segregation distortion in *Drosophila* hybrids. *Science* 323(5912):376–379.
- Phifer-Rixey M, Nachman MW. 2015. Insights into mammalian biology from the wild house mouse *Mus musculus*. *Elife* 4:e05959.
- Pialek J, Vyskocilova M, Bimova B, Havelkova D, Pialkova J, Dufkova P, Bencova V, Dureje L, Albrecht T, Hauffe HC, et al. 2007. Development of unique house mouse resources suitable for evolutionary studies of speciation. *J Hered.* 99(1):34–44.
- Powers NR, Parvanov ED, Baker CL, Walker M, Petkov PM, Paigen K. 2016. The meiotic recombination activator PRDM9 trimethylates both H3K36 and H3K4 at recombination hotspots in vivo. *PLoS Genet.* 12(6):e1006146.
- Presgraves DC. 2018. Evaluating genomic signatures of “the large X-effect” during complex speciation. *Mol Ecol.* 27(19):3822–3830.
- Presgraves DC. 2008. Sex chromosomes and speciation in *Drosophila*. *Trends Genet.* 24(7):336–343.
- Presgraves DC, Balagopalan L, Abmayr SM, Orr HA. 2003. Adaptive evolution drives divergence of a hybrid inviability gene between two species of *Drosophila*. *Nature* 423(6941):715–719.
- Saitou N, Nei M. 1987. The neighbor-joining method: a new method for reconstructing phylogenetic trees. *Mol Biol Evol.* 4(4):406–425.
- Salcedo T, Galdes A, Nachman MW. 2007. Nucleotide variation in wild and inbred mice. *Genetics* 177(4):2277–2291.
- She J, Bonhomme F, Boursot P, Thaler L, Catzeflis F. 1990. Molecular phylogenies in the genus *Mus*: comparative analysis of electrophoretic, scnDNA hybridization, and mtDNA RFLP data. *Biol J Linn Soc.* 41(1–3):83–103.
- Schilthuis M, Giesbers MC, Beukeboom LW. 2011. Haldane’s rule in the 21st century. *Heredity* 107(2):95–102.
- Schneider CA, Rasband WS, Eliceiri KW. 2012. NIH Image to ImageJ: 25 years of image analysis. *Nat Methods.* 9(7):671–675.
- Schwahn DJ, Wang RJ, White MA, Payseur BA. 2018. Genetic dissection of hybrid male sterility across stages of spermatogenesis. *Genetics* 210(4):1453–1465.
- Smagulova F, Brick K, Pu Y, Camerini-Otero RD, Petukhova GV. 2016. The evolutionary turnover of recombination hot spots contributes to speciation in mice. *Genes Dev.* 30(3):266–280.
- Smagulova F, Gregoretti IV, Brick K, Khil P, Camerini-Otero RD, Petukhova GV. 2011. Genome-wide analysis reveals novel molecular features of mouse recombination hotspots. *Nature* 472(7343):375–378.
- Smith GR, Nambiar M. 2020. New solutions to old problems: molecular mechanisms of meiotic crossover control. *Trends Genet.* 36(5):337–346.
- Spruce C, Dlamini S, Ananda G, Bronkema N, Tian H, Paigen K, Carter GW, Baker CL. 2020. HELLS and PRDM9 form a pioneer complex to open chromatin at meiotic recombination hot spots. *Genes Dev.* 34(5–6):398–412.
- Storchova R, Gregorova S, Buckiova D, Kyselova V, Divina P, Forejt J. 2004. Genetic analysis of X-linked hybrid sterility in the house mouse. *Mamm Genome.* 15(7):515–524.
- Tamura K, Nei M, Kumar S. 2004. Prospects for inferring very large phylogenies by using the neighbor-joining method. *Proc Natl Acad Sci U S A.* 101(30):11030–11035.
- Teeter KC, Payseur BA, Harris LW, Bakewell MA, Thibodeau LM, O’Brien JE, Krenz JG, Sans-Fuentes MA, Nachman MW, Tucker PK. 2007. Genome-wide patterns of gene flow across a house mouse hybrid zone. *Genome Res.* 18(1):67–76.
- Teeter KC, Thibodeau LM, Gompert Z, Buerkle CA, Nachman MW, Tucker PK. 2010. The variable genomic architecture of isolation between hybridizing species of house mice. *Evolution* 64(2):472–485.
- Ting CT, Tsaou SC, Wu ML, Wu CI. 1998. A rapidly evolving homeobox at the site of a hybrid sterility gene. *Science* 282(5393):1501–1504.
- Trachtulec Z, Mňuková-Fajdelová M, Hamvas RMJ, Gregorová S, Mayer WE, Lehrach HR, Vincik V, Forejt J, Klein J. 1997. Isolation of candidate hybrid sterility 1 genes by cDNA selection in a 1.1 megabase pair region on mouse chromosome 17. *Mamm Genome.* 8(5):312–316.
- Tucker P, Sage R, Warner J, Wilson A, Eicher E. 1992. Abrupt cline for sex chromosomes in a hybrid zone between two species of mice. *Evolution* 46(4):1146–1163.
- Turner LM, Harr B. 2014. Genome-wide mapping in a house mouse hybrid zone reveals hybrid sterility loci and Dobzhansky-Muller interactions. *Elife* 3:e02504.
- Turner LM, Schwahn DJ, Harr B. 2012. Reduced male fertility is common but highly variable in form and severity in a natural house mouse hybrid zone. *Evolution* 66(2):443–458.
- Vara C, Capilla L, Ferretti L, Ledda A, Sánchez-Guillén RA, Gabriel SI, Albert-Lizandra G, Florit-Sabater B, Bello-Rodríguez J, Ventura J, et al. 2019. PRDM9 diversity at fine geographical scale reveals contrasting evolutionary patterns and functional constraints in natural populations of house mice. *Mol Biol Evol.* 36(8):1686–1700.

- Vyskocilova M, Prazanova G, Pialek J. 2009. Polymorphism in hybrid male sterility in wild-derived *Mus musculus musculus* strains on proximal chromosome 17. *Mamm Genome*. 20:83–91.
- Vyskočilová M, Trachtulec Z, Forejt J, Piálek J. 2005. Does geography matter in hybrid sterility in house mouse? *Biol J Linn Soc*. 84(3):663–674.
- Wang L, Valiskova B, Forejt J. 2018. Cisplatin-induced DNA double-strand breaks promote meiotic chromosome synapsis in PRDM9-controlled mouse hybrid sterility. *Elife* 7:e42511.
- Wang RJ, White MA, Payseur BA. 2015. The pace of hybrid incompatibility evolution in house mice. *Genetics* 201(1):229–242.
- White MA, Steffy B, Wiltshire T, Payseur BA. 2011. Genetic dissection of a key reproductive barrier between nascent species of house mice. *Genetics* 189(1):289–304.
- White MA, Stubbings M, Dumont BL, Payseur BA. 2012. Genetics and evolution of hybrid male sterility in house mice. *Genetics* 191(3):917–934.
- Wojtasz L, Cloutier JM, Baumann M, Daniel K, Varga J, Fu J, Anastassiadis K, Stewart AF, Remenyi A, Turner JMA, et al. 2012. Meiotic DNA double-strand breaks and chromosome asynapsis in mice are monitored by distinct HORMAD2-independent and -dependent mechanisms. *Genes Dev*. 26(9):958–973.
- Wojtasz L, Daniel K, Roig I, Bolcun-Filas E, Xu H, Boonsanay V, Eckmann CR, Cooke HJ, Jasin M, Keeney S, et al. 2009. Mouse HORMAD1 and HORMAD2, two conserved meiotic chromosomal proteins, are depleted from synapsed chromosome axes with the help of TRIP13 AAA-ATPase. *PLoS Genet*. 5(10):e1000702.
- Wu H, Mathioudakis N, Diagouraga B, Dong A, Dombrowski L, Baudat F, Cusack S, de Massy B, Kadlec J. 2013. Molecular basis for the regulation of the H3K4 methyltransferase activity of PRDM9. *Cell Rep*. 5(1):13–20.
- Yamada S, Kim S, Tischfield SE, Jasin M, Lange J, Keeney S. 2017. Genomic and chromatin features shaping meiotic double-strand break formation and repair in mice. *Cell Cycle* 16(20):1870–1884.
- Yang H, Wang JR, Didion JP, Buus RJ, Bell TA, Welsh CE, Bonhomme F, Yu AH, Nachman MW, Pialek J, et al. 2011. Subspecific origin and haplotype diversity in the laboratory mouse. *Nat Genet*. 43(7):648–655.